Bulletin of Mathematical Biology (1999) **61**, 507–530
Article No. bulm.1999.0095
Available online at http://www.idealibrary.com on IDEAL®

Bursting, Chaos and Birhythmicity Originating from Self-modulation of the Inositol 1,4,5-trisphosphate Signal in a Model for Intracellular Ca^{2+} Oscillations

GÉRALD HOUART, GENEVIÈVE DUPONT AND ALBERT GOLDBETER
Unité de Chronobiologie Théorique, Faculté des Sciences,
Université Libre de Bruxelles, Campus Plaine,
C.P. 231, B-1050 Brussels,
Belgium
E-mail: agoldbet@ulb.ac.be

We investigate the various types of complex Ca^{2+} oscillations which can arise in a model based on the mechanism of Ca^{2+}-induced Ca^{2+} release (CICR), that takes into account the Ca^{2+}-stimulated degradation of inositol 1,4,5-trisphosphate ($InsP_3$) by a 3-kinase. This model was previously proposed in the course of an investigation of plausible mechanisms capable of generating complex Ca^{2+} oscillations (Borghans *et al*., 1997). Besides simple periodic behavior, this model for cytosolic Ca^{2+} oscillations in nonexcitable cells shows complex oscillatory phenomena like bursting or chaos. We show that the model also admits a coexistence between two stable regimes of sustained oscillations (birhythmicity). The occurrence of these various modes of oscillatory behavior is analysed by means of bifurcation diagrams. Complex oscillations are characterized by means of Poincaré sections, power spectra and Lyapounov exponents. The results point to the role of self-modulation of the $InsP_3$ signal by 3-kinase as a possible source for complex temporal patterns in Ca^{2+} signaling.

1. INTRODUCTION

A large variety of cell types display Ca^{2+} oscillations after stimulation by an extracellular agonist such as a hormone or a neurotransmitter (Berridge, 1993, 1997; Berridge and Dupont, 1994; Thomas *et al*., 1996). In most cell types, these oscillations take the form of repetitive sharp spikes in the level of cytosolic Ca^{2+}. Typically, the cytosolic Ca^{2+} concentration varies from less than 0.1 μM up to 1 μM with a periodicity that ranges from a few seconds to 30 minutes. In nearly all cell types the frequency of Ca^{2+} oscillations is seen to increase with the level of stimulation, a phenomenon that strongly suggests that the external signal is encoded in terms of the temporal pattern of Ca^{2+} oscillations. Although the pathway between the successive Ca^{2+} spikes and the cellular response remains poorly understood in most cell types, there is increasing evidence pointing to a physiological role for these

0092-8240/99/030507 + 24 $30.00/0

oscillations (Ozil and Swann, 1995; Thomas *et al*., 1996). Of particular interest in this respect is the recent demonstration that Ca^{2+} oscillations of appropriate frequency may increase the efficiency and specificity of gene expression (Dolmetsch *et al*., 1998; Li *et al*., 1998).

In the vast majority of cells, the external stimulus triggers the synthesis of inositol 1,4,5-trisphosphate ($InsP_3$), an intracellular messenger known to bind to receptors located on the membrane of the endoplasmic reticulum, thereby initiating the release of Ca^{2+} into the cytosol. As the release of Ca^{2+} through the $InsP_3$ receptor/Ca^{2+} channel is activated by Ca^{2+} itself, Ca^{2+} release in the cytosol possesses an autocatalytic nature which is responsible for Ca^{2+} oscillations under appropriate conditions. This phenomenon by which cytosolic Ca^{2+} activates its own release from the intracellular stores is known as Ca^{2+}-induced Ca^{2+} release (CICR). CICR was originally described for muscle (Endo *et al*., 1970) and cardiac cells (Fabiato and Fabiato, 1975), but was later found to occur in a variety of other cell types (Berridge, 1993). Numerous models based on CICR have been proposed to account for the existence and for the main properties of these oscillations (for reviews, see Dupont and Goldbeter, 1992; Chay, 1993a; Sneyd *et al*., 1995; Goldbeter, 1996; Tang *et al*., 1996; Dupont, 1999).

In some cell types, particularly in hepatocytes, complex Ca^{2+} oscillations reminiscent of the bursting-like behavior displayed by many electrically excitable cells have been observed in response to stimulation by specific agonists (Green *et al*., 1993; Marrero *et al*., 1994). As these cells are not electrically excitable, it is likely that these complex Ca^{2+} oscillations rely on the interplay between two intracellular mechanisms capable of destabilizing the steady state. Some theoretical models have been proposed to account for such complex Ca^{2+} oscillations (Chay *et al*., 1995; Shen and Larter, 1995; Borghans *et al*., 1997). Among these models, the one based on the interplay between CICR at the level of the $InsP_3$ receptor and the Ca^{2+}-stimulated $InsP_3$ degradation (Borghans *et al*., 1997) appears to be of particular interest. First, this model is based on the well characterized stimulation by Ca^{2+} of the activity of inositol 1,4,5-trisphosphate 3-kinase, one of the $InsP_3$ metabolizing enzymes (Takazawa *et al*., 1989, 1990). Second, this model can generate a large variety of dynamical behaviors, including deterministic chaos and Ca^{2+} oscillations of the bursting type that much resemble experimental observations [see Figs 1 and 8 of Borghans *et al*. (1997) for a comparison between experimental and theoretical oscillations].

The goal of the present study is to investigate in more detail the conditions in which complex oscillatory phenomena occur in that model, and to characterize more thoroughly the various modes of dynamical behavior that can be obtained, i.e., simple periodic oscillations of the limit cycle type, bursting, quasiperiodic oscillations, and deterministic chaos. In Section 2, we first briefly present the model previously proposed for complex Ca^{2+} oscillations. In Section 3, we investigate the relationship between the level of stimulation and the frequency of Ca^{2+} oscillations in the case of simple periodic behavior to determine whether this model can account

for the observed increase in the frequency of Ca^{2+} oscillations with the degree of stimulation. Two antagonistic effects are indeed at play: an increase in $InsP_3$ is expected to lead to an increase in the frequency of Ca^{2+} spikes, but at the same time the $InsP_3$-induced rise in Ca^{2+} will also lead to increased $InsP_3$ hydrolysis due to the Ca^{2+} activation of the $InsP_3$ 3-kinase. In Section 4, we present the various types of complex dynamical behavior that can be exhibited by the model. Bursting, chaos and quasiperiodicity are considered in turn. In Section 5, we study by means of bifurcation diagrams how these complex temporal patterns appear and disappear as a function of the degree of stimulation. We also show that the model can display birhythmicity, i.e., the coexistence between two stable limit cycles. In Section 6, we characterize these dynamical behaviors by means of return maps, power spectra and evaluation of Lyapounov exponents. The results are discussed in Section 7, both with respect to their possible physiological significance and to the potential role of the Ca^{2+}-activated $InsP_3$ degradation as a source for complex Ca^{2+} oscillations.

2. Model for Ca^{2+} Oscillations involving Ca^{2+}-activated $InsP_3$ Degradation

The model used in the present study is an extension of the minimal model proposed by Dupont and Goldbeter (1993) to account for the existence of simple Ca^{2+} oscillations in response to extracellular stimulation. The original model only involves two variables, namely cytosolic and intravesicular Ca^{2+} concentrations. The release of Ca^{2+} from the internal stores into the cytosol is activated by $InsP_3$ and cytosolic Ca^{2+}; such an autocatalytic process of $InsP_3$-sensitive CICR is at the core of the oscillatory mechanism. Oscillations of Ca^{2+} in this basic model do not require, and are not accompanied by, a periodic variation in $InsP_3$, in agreement with observations which show that repetitive Ca^{2+} spikes may occur in the presence of a constant level of $InsP_3$ (Wakui *et al*., 1989; Berridge, 1993). However, although it is highly plausible that CICR is the primary oscillatory mechanism, the concentration of $InsP_3$ most probably evolves nonmonotonously in the course of time. $InsP_3$, which is a second messenger, is synthesized by phospholipase C (PLC) in response to external stimulation and metabolized into $InsP_2$ by a 5-phosphatase and into $InsP_4$ by a 3-kinase (Takazawa *et al*., 1990; Berridge, 1993). An oscillatory variation of $InsP_3$ could result from the control of any of these three enzymes by Ca^{2+}. In support of such a possibility, some experiments report that the activity of PLC is stimulated by Ca^{2+} (Renard *et al*., 1987); the activation of the 3-kinase by Ca^{2+} is even better documented (Takazawa *et al*., 1989, 1990).

Stimulation of PLC activity by Ca^{2+} has been taken into account in some theoretical models (Meyer and Stryer, 1988; Keizer and De Young, 1992; Shen and Larter, 1995). One of these models (Shen and Larter, 1995) can exhibit bursting-type oscillations (also called mixed-mode oscillations) as well as chaos; the level of cytosolic Ca^{2+} returns in both cases to its basal value between successive Ca^{2+}

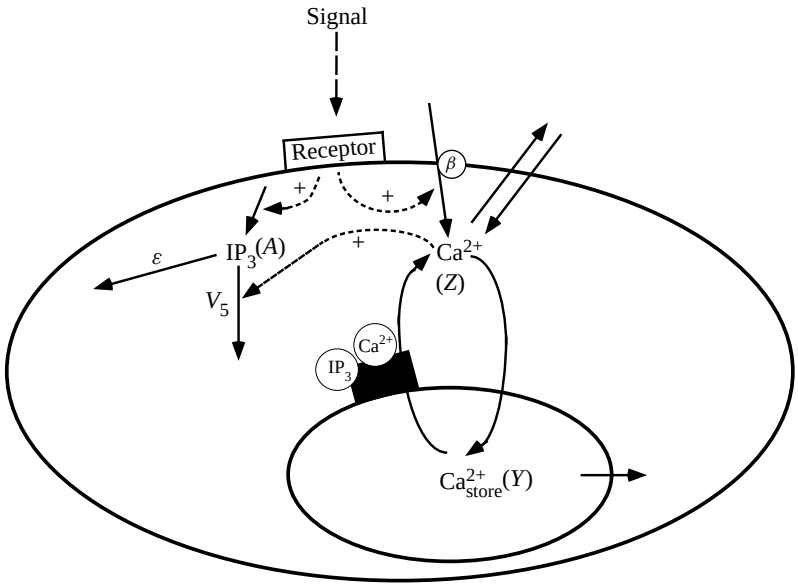

Figure 1. Schematic representation of the model based on the interplay between CICR and the Ca^{2+}-stimulated degradation of $InsP_3$ (see text for details). Besides simple periodic oscillations, this model can produce complex Ca^{2+} oscillations including bursting, chaos, quasiperiodic behavior, as well as birhythmicity.

spikes. Such a temporal pattern does not resemble the behavior seen in hepatocytes stimulated by various agonists such as cAMP (Capiod *et al*., 1991), taurolithocholate 3-sulfate (Marrero *et al*., 1994), diadenosine 5′, 5‴-P^1P^4-tetraphosphate (Green *et al*., 1993), ATP or both ATP and cAMP (Dixon *et al*., 1993, 1995; Green *et al*., 1994). With these agonists, bursting in hepatocytes takes the form of a switch between a silent phase and an active phase made of small-amplitude Ca^{2+} oscillations around an elevated Ca^{2+} level. The latter type of complex oscillations can be obtained in numerical simulations when extending the model based on CICR to take into account the stimulation of $InsP_3$ 3-kinase activity by the Ca^{2+}/calmodulin complex, as shown by Borghans *et al*. (1997). The present paper aims at investigating in further detail the occurrence of complex oscillations in this extended model, which also incorporates Ca^{2+} pumping into the stores, Ca^{2+} exchange with the external medium, as well as stimulus-activated Ca^{2+} entry (Dupont and Goldbeter, 1993; Borghans *et al*., 1997).

The model, schematized in Fig. 1, contains three variables, namely the concentrations of free Ca^{2+} in the cytosol (Z) and in the internal pool (Y), and the $InsP_3$ concentration (A). The time evolution of these variables is governed by the following ordinary differential equations:

$$\frac{dZ}{dt} = V_{in} - V_2 + V_3 + k_f Y - kZ \tag{1a}$$

$$\frac{dY}{dt} = V_2 - V_3 - k_f Y \tag{1b}$$

$$\frac{dA}{dt} = \beta V_4 - V_5 - \varepsilon A, \tag{1c}$$

where

$$V_{in} = V_0 + V_1\beta \tag{2}$$

$$V_2 = V_{M2}\frac{Z^2}{K_2^2 + Z_2} \tag{3}$$

$$V_3 = V_{M3}\frac{Z^m}{K_Z^m + Z^m}\frac{Y^2}{K_Y^2 + Y^2}\frac{A^4}{K_A^4 + A^4} \tag{4}$$

$$V_5 = V_{M5}\frac{A^p}{K_5^p + A^p}\frac{Z^n}{K_d^n + Z^n}. \tag{5}$$

In these equations, V_0 refers to a constant input of Ca^{2+} from the extracellular medium and V_1 is the maximum rate of stimulus-induced influx of Ca^{2+} from the extracellular medium. Parameter β reflects the degree of stimulation of the cell by an agonist and thus only varies between 0 and 1. The rates V_2 and V_3 refer, respectively, to pumping of cytosolic Ca^{2+} into the internal stores and to the release of Ca^{2+} from these stores into the cytosol in a process activated by cytosolic calcium (CICR); V_{M2} and V_{M3} denote the maximum values of these rates. Parameters K_2, K_Y, K_Z and K_A are threshold constants for pumping, release, and activation of release by Ca^{2+} and by $InsP_3$; k_f is a rate constant measuring the passive, linear leak of Y into Z; k relates to the assumed linear transport of cytosolic Ca^{2+} into the extracellular medium; V_4 is the maximum rate of stimulus-induced synthesis of $InsP_3$. V_5 is the rate of phosphorylation of $InsP_3$ by the 3-kinase; it is characterized by a maximum value V_{M5} and a half-saturation constant K_5.

The fact that the 3-kinase is stimulated by Ca^{2+} — through the formation of a Ca^{2+}/calmodulin complex which is not explicitly considered in the model — is taken into account through a term of the Hill form, with a threshold Ca^{2+} level equal to K_d. That $InsP_3$ can also be metabolized in a Ca^{2+}-independent manner by the 5-phosphatase is reflected by the term $-\varepsilon A$, which can be assumed to be of the first-order given that the latter enzyme has a low affinity for its substrate, of the order of 10 μM (Verjans *et al.*, 1992). This term is significant when the level of cytosolic Ca^{2+} is very low, i.e., when the term V_5 becomes negligible in equation (1c). Equations (3–5) allow for cooperativity in the kinetics of Ca^{2+} release, Ca^{2+} pumping and $InsP_3$ phosphorylation by the 3-kinase; m, n and p are Hill coefficients related to the cooperative processes. Experimental evidence indicates that the 3-kinase behaves as a Michaelian enzyme with respect to its substrate $InsP_3$, hence $p = 1$ (Takazawa *et al.*, 1989). The results indicate that complex oscillations, including chaos, can occur both in the presence ($p > 1$) or absence ($p = 1$) of cooperativity in the kinetics of 3-kinase.

3. Dependence of the Frequency of Simple Periodic Ca^{2+} Oscillations on the Degree of Stimulation

Intracellular Ca^{2+} oscillations take the form of abrupt spikes, sometimes preceded by a gradual increase in cytosolic Ca^{2+}. They only occur in a range bounded by two critical values of the stimulation level, with the frequency of the spikes increasing with the intensity of the stimulus. These properties are well accounted for by the model, as illustrated in Fig. 2. Figure 2(a) shows typical Ca^{2+} oscillations generated by the model. Here, in contrast to the original model (Dupont and Goldbeter, 1993), these oscillations are necessarily accompanied by periodic variations in the level of $InsP_3$. As can be expected from the regulations considered, the peak in $InsP_3$ slightly precedes the peak in cytosolic Ca^{2+}. The bifurcation diagram [Fig. 2(b)] shows the steady-state value of cytosolic Ca^{2+} (Z), when it is stable, or the maxima and minima reached during oscillations when it is unstable. As in the minimal model for Ca^{2+} oscillations (Dupont and Goldbeter, 1993), the steady-state value of cytosolic Ca^{2+} increases with the level of stimulation, β, and the amplitude of the oscillations remains practically constant over the whole oscillatory domain bounded by two supercritical Hopf bifurcation points. The frequency of oscillations increases with the level of external stimulation [Fig. 2(c)].

The relationship between the level of stimulation and the frequency of Ca^{2+} oscillations shown in Fig. 2(c) is in good qualitative agreement with experimental observations. However, numerical simulations of the model defined by equations (1)–(5) show that this is not always the case. For example, depending on the maximal rate of phosphorylation of $InsP_3$ by the 3-kinase (V_{M5}), we observe that the frequency of the oscillations increases monotonously with the degree of stimulation β (as in Fig. 2 and in Fig. 3, curve a, where the value of V_{M5} is small) or may pass through a minimum as a function of β (as in Fig. 3, curve b, in which V_{M5} is larger). In the model, increasing the level of stimulation triggers a rise first in the rate of synthesis and then in the rate of degradation of $InsP_3$ (due to the enhanced stimulation of the 3-kinase by Ca^{2+}). This explains why, depending on relative parameter values, qualitatively distinct relationships between the degree of stimulation and the frequency of Ca^{2+} oscillations can be obtained.

These different relationships are illustrated in Fig. 3 for distinct values of parameter V_{M5}, which represents the maximum rate of $InsP_3$ degradation by 3-kinase. For high values of V_{M5} (curve b), the latter enzyme significantly regulates the level of $InsP_3$, which does not vary much with the level of stimulation (β). The Ca^{2+} concentration indeed rises as a function of β, and thus $InsP_3$ metabolism is enhanced (through the activation of $InsP_3$ 3-kinase). Hence, at the beginning of the oscillatory domain, the increase in cytosolic Ca^{2+} due to the rise in β [equation (2)] produces a slight decrease in $InsP_3$: the rate of Ca^{2+} release then decreases as β rises and, as a consequence, the frequency decreases. Beyond $\beta = 0.16$, however, a switch occurs: the synthesis of $InsP_3$ rises more with β than the Ca^{2+}-induced degradation of $InsP_3$, so that the frequency of oscillations rises as β increases. For another set of

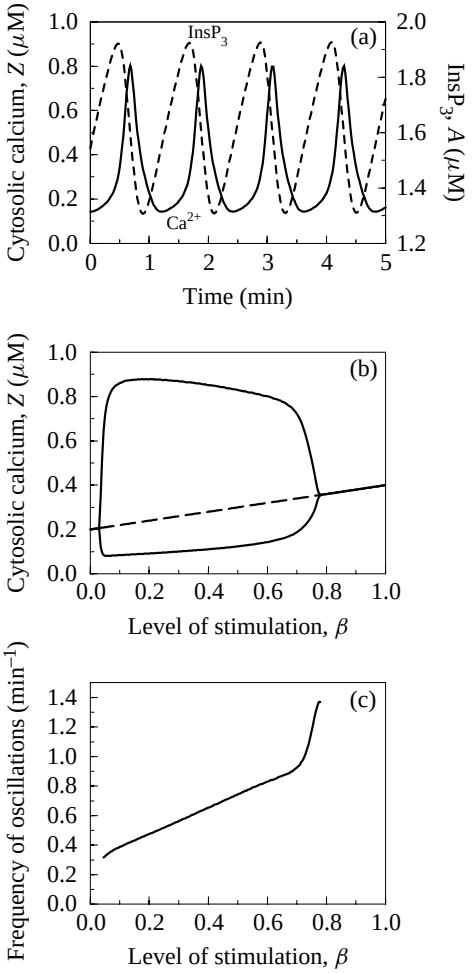

Figure 2. Simple oscillations of Ca^{2+} and $InsP_3$ in the model based on the interplay between CICR and the Ca^{2+}-stimulated degradation of $InsP_3$. (a) Temporal evolution of the concentrations of cytosolic calcium (Z, solid line) and $InsP_3$ (A, dashed line). The curves have been obtained by numerical integration of the model defined by equations (1)–(5) with the following parameter values: $\beta = 0.6$, $\varepsilon = 0.1$ min^{-1}, $k = 10$ min^{-1}, $K_2 = 0.1\,\mu$M, $K_A = 0.2\,\mu$M, $K_d = 0.4\,\mu$M, $k_f = 1$ min^{-1}, $K_5 = 1\,\mu$M, $K_Y = 0.2\,\mu$M, $K_Z = 0.5\,\mu$M, $V_0 = V_1 = 2\,\mu$M min^{-1}, $V_{M5} = 5\,\mu$M min^{-1}, $V_{M2} = 6\,\mu$M min^{-1}, $V_{M3} = 20\,\mu$M min^{-1}, $V_4 = 2\,\mu$M min^{-1}, $m = p = 2$, $n = 4$. (b) Bifurcation diagram giving the steady state (stable or unstable) and the envelope of the oscillations in Z as a function of β for the same set of parameter values. (c) Relationship between the frequency of Ca^{2+} oscillations and the level of stimulation in the same conditions.

parameter values, the frequency can even decrease in the entirety of the oscillatory domain as the level of stimulation increases (data not shown). In contrast, for lower values of V_{M5} (curve a), the rate of $InsP_3$ synthesis by PLC exceeds the activity of 3-kinase in the whole oscillatory domain. Thus, even at low stimulation level, the frequency always increases with β, in agreement with experimental observations.

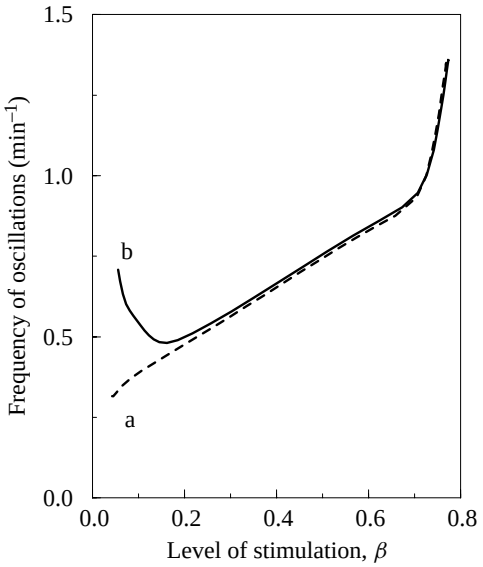

Figure 3. Different relationships between the frequency of Ca^{2+} oscillations and the level of stimulation in the model based on the interplay between CICR and the Ca^{2+}-stimulated degradation of $InsP_3$. Parameter values are the same as in Fig. 2, except for V_{M5} which is equal to 5 μM min^{-1} in (a) — as in Fig. 2(c) — and 15 μM min^{-1} in (b).

As an inverse relationship between the frequency of Ca^{2+} oscillations and the level of stimulation has never been experimentally reported, the present theoretical results suggest that Ca^{2+} oscillations are not primarily affected by variations in the level of $InsP_3$ due to the stimulation of 3-kinase activity by Ca^{2+}. This result corroborates the view that in most cell types [except some cells like hippocampal neurons; see Mailleux *et al*. (1991)], in physiological conditions, $InsP_3$ metabolism is mainly carried out by the $InsP_3$ 5-phosphatase — the action of which is reflected by the term $-\varepsilon A$ in equation (1c) — because of the high maximum activity of this enzyme relative to that of the 3-kinase (De Smedt *et al*., 1997; Dupont and Erneux, 1997). The present results suggest, however, that unusual relationships between the level of stimulation and the frequency of Ca^{2+} oscillations could be observed in cells overexpressing $InsP_3$ 3-kinase.

4. COMPLEX CA^{2+} OSCILLATIONS: BURSTING, QUASIPERIODICITY AND CHAOS

Although simple Ca^{2+} oscillations resembling those shown in Fig. 2 are usually observed in response to external stimulation, complex oscillations have also been reported in experiments performed with hepatocytes responding to a variety of agonists (Green *et al*., 1993; Marrero *et al*., 1994). A detailed investigation of the dynamic behavior of the model in parameter space allowed us to uncover re-

Table 1. Parameter values corresponding to the various types of complex oscillatory behavior observed in the model defined by equations (1)–(5).

Parameters	Bursting	Chaos	Quasiperiodicity
β	0.46	0.65	0.51
K_2 (μM)	0.1	0.1	0.1
K_5 (μM)	1	0.3194	0.3
K_A (μM)	0.1	0.1	0.2
K_d (μM)	0.6	1	0.5
K_Y (μM)	0.2	0.3	0.2
K_Z (μM)	0.3	0.6	0.5
k (min^{-1})	10	10	10
k_f (min^{-1})	1	1	1
ε (min^{-1})	1	13	0.1
n	2	4	4
m	4	2	2
p	1	1	2
V_0 ($\mu\text{M min}^{-1}$)	2	2	2
V_1 ($\mu\text{M min}^{-1}$)	2	2	2
V_{M2} ($\mu\text{M min}^{-1}$)	6	6	6
V_{M3} ($\mu\text{M min}^{-1}$)	20	30	20
V_{M4} ($\mu\text{M min}^{-1}$)	2.5	3	5
V_{M5} ($\mu\text{M min}^{-1}$)	30	50	30

gions of complex Ca^{2+} oscillations, including bursting, chaos and quasiperiodicity. Three sets of parameter values corresponding to these modes of complex oscillatory behavior are listed in Table 1.

The different types of oscillations are illustrated in Fig. 4, both as a function of time (left column) and in the phase space (right column). For oscillations of the bursting type, a large-amplitude Ca^{2+} spike is followed by smaller Ca^{2+} variations around a plateau level [Fig. 4(a)]. The corresponding attractor is plotted in Fig. 4(d). After a first, large Ca^{2+} spike, $InsP_3$ is metabolized by the 3-kinase which has been massively activated by Ca^{2+}; enough $InsP_3$, however, remains to allow for some repetitive Ca^{2+}-releasing activity through CICR, producing small-amplitude spikes, up to a point where the levels of cytosolic and intravesicular Ca^{2+} are both too low to activate Ca^{2+} release.

As illustrated in Fig. 4(b), aperiodic, chaotic oscillations are usually of reduced amplitude and never undergo large excursions in the phase space [see Fig. 4(e)], as compared to the case of bursting [Fig. 4(a) and (d)]. The irregularity of the oscillations shows up both in the amplitude and in the time interval between successive Ca^{2+} spikes. From a practical point of view, these intrinsically irregular oscillations might be hard to distinguish from a noisy experimental record of low-amplitude periodic Ca^{2+} oscillations. In this respect, it is of interest that an analysis of experimentally obtained time series of Ca^{2+} oscillations showed that in some

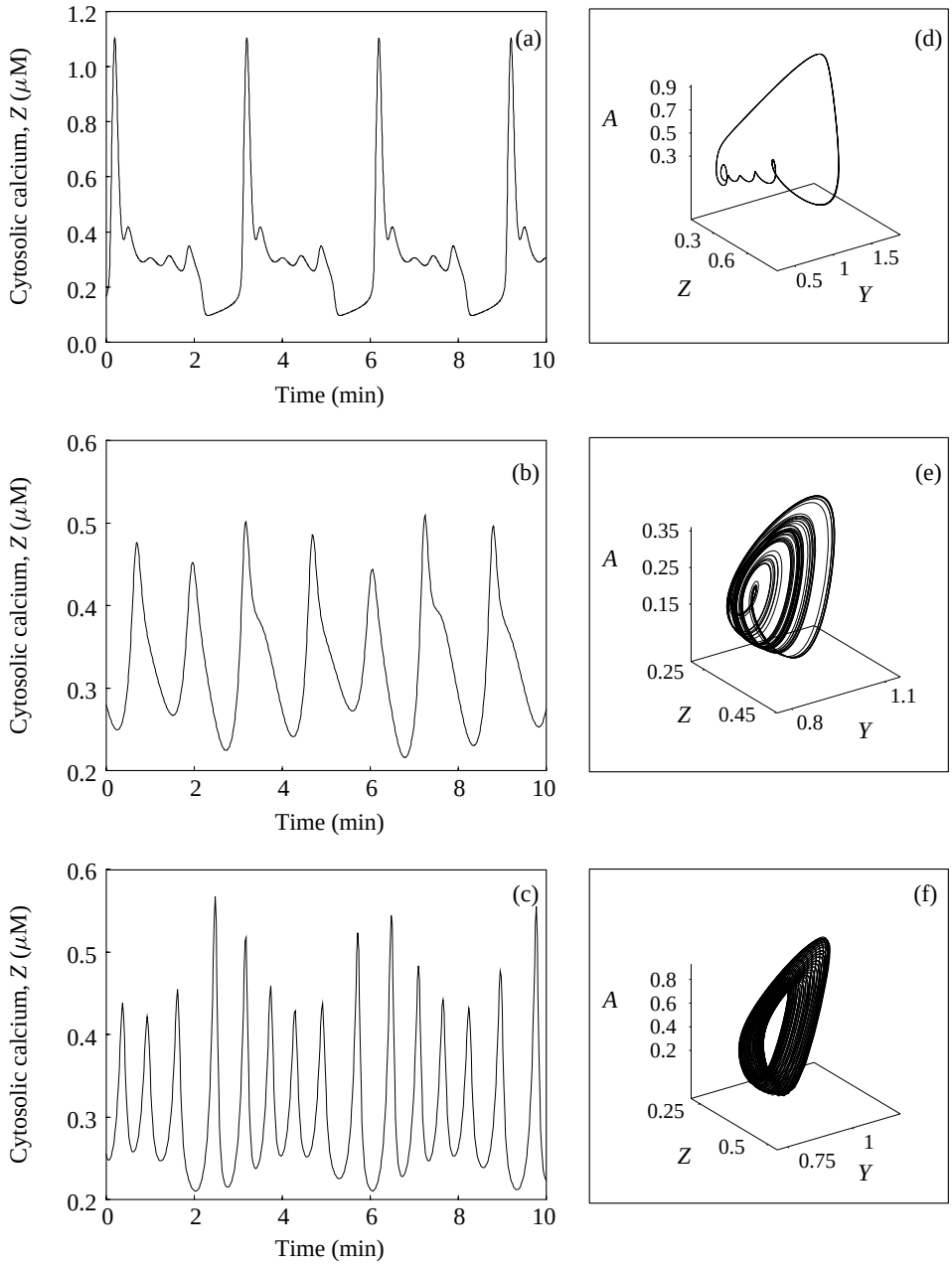

Figure 4. Various types of complex Ca^{2+} oscillations that can be obtained in the model based on the interplay between CICR and the Ca^{2+}-stimulated degradation of $InsP_3$. From top to bottom, these complex behaviors correspond to bursting, chaos and quasiperiodicity. The panels on the left show the time evolution of cytosolic Ca^{2+} concentration while the right panels show the corresponding attractors in the phase space. Results have been obtained by numerical integration of the model defined by equations (1)–(5) for the three sets of parameter values listed in Table 1, where the first column refers to (a) and (d), the second column to (b) and (e), and the third column to (c) and (f).

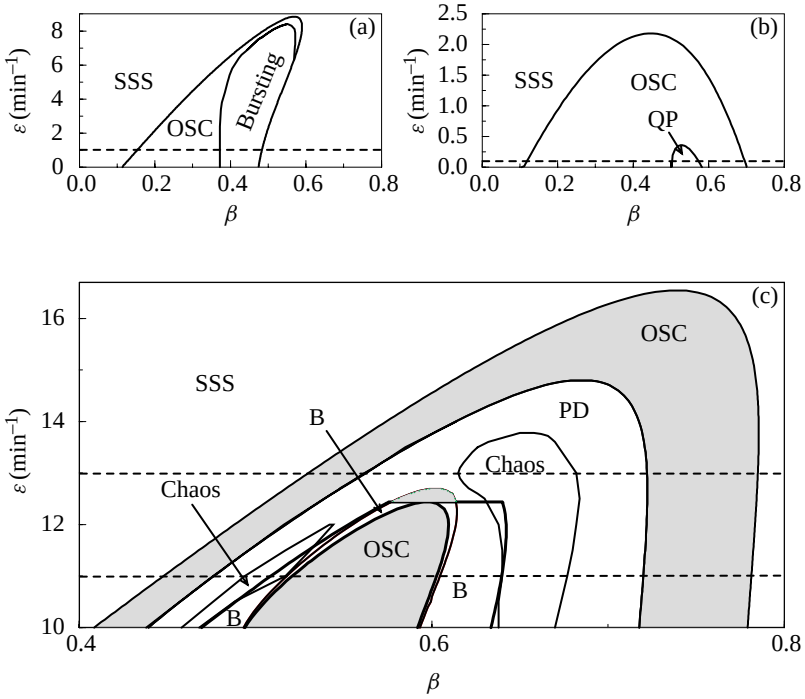

Figure 5. Stability diagrams showing the domains of (a) bursting, (b) quasiperiodicity, and (c) chaos as well as other modes of complex oscillatory behavior. Notations are: SSS for stable steady state, OSC for simple periodic oscillations, QP for quasiperiodicity, PD for the beginning of the period-doubling sequences, CHAOS for areas of chaotic dynamics, and B for regions of birhythmicity. The diagrams have been established by numerical integration of equations (1)–(5) with the parameter values listed in the first, second and third columns of Table 1 for (a), (c) and (b), respectively. The four horizontal dashed lines represent sections through the domains of distinct dynamic behaviors, which correspond to the bifurcation diagrams presented in Fig. 6.

cases the Ca^{2+} dynamics can be casted into low-dimensional chaos (Strizhak *et al.*, 1995). A typical strange attractor corresponding to the chaotic dynamics of Fig. 4(b) is shown in Fig. 4(e). Finally, Fig. 4(c) shows an example of quasiperiodic oscillations obtained with the model. Such a kind of oscillatory behavior, characterized by the existence of multiple frequencies (Bergé *et al.*, 1984), has been less often reported for biochemical systems. Although the time series greatly resemble the chaotic one, quasiperiodicity is easily recognizable in phase space in which all trajectories are concentrated on a torus [Fig. 4(f)].

The domains in which the various modes of complex oscillatory behavior occur in the model are illustrated in Fig. 5 by the stability diagrams established as a function of parameters ε and β which measure, respectively, the degradation of $InsP_3$ by the 5-phosphatase and the degree of cell stimulation. Figure 5(a)–(c) correspond to the three sets of parameter values listed in Table 1. In Fig. 5(a), a domain of bursting is nested within the domain of simple periodic behavior. In Fig. 5(b),

a small domain of quasiperiodicity is nested within a domain of simple periodic oscillations. In Fig. 5(c), multiple nested domains are found in which, from the center to the periphery, simple periodic oscillations exhibiting a small shoulder (see thin curve in the left panel of Fig. 8) are followed, successively, by birhythmicity, chaos, period-doublings, simple periodic oscillations, and stable steady states.

In the next section, we will discuss from a dynamical point of view the origin of these various modes of complex oscillatory behavior. To this end, we have chosen to use the particular sets of parameter values listed in Table 1 for each mode of complex oscillations, keeping β free to vary as bifurcation parameter.

5. Bifurcation Diagrams for the Three Types of Complex Oscillations

5.1. ***Bursting.*** Figure 6(a) shows a typical bifurcation diagram illustrating the origin of bursting in the model based on the interplay between CICR and Ca^{2+}-stimulated degradation of $InsP_3$. This bifurcation diagram represents a horizontal section (dashed line) through the diagram of Fig. 5(a). The level of stimulation, β, is considered as the most relevant bifurcation parameter since it is more readily amenable to experimental manipulation. Shown are the steady state, if stable, and the maxima and minima of cytosolic Ca^{2+} (Z) reached during oscillations when the steady state is unstable. The first limit cycle arises through a Hopf bifurcation at $\beta = 0.153$ and loses its stability at $\beta = 0.369$. A rapid sequence of bursting states can be seen for increasing stimulation levels; in this region of the bifurcation diagram, the number of peaks during the active phase of bursting increases with β. The complex oscillations disappear abruptly, and the steady state becomes stable again at $\beta = 0.483$. Figure 7 shows that, at this critical point, the period of oscillations tends to infinity, a feature characteristic of a homoclinic bifurcation. Also noticeable in Fig. 7 is the fact that the period increases in a stepwise manner with β, because the number of spikes in the plateau phase increases at each step. Figure 6(a) and subsequent bifurcation diagrams have been obtained by numerical integration of equations (1)–(5). Similar results have also been obtained in part using the program AUTO (Doedel, 1981), but only the first bifurcations were found with this method.

5.2. ***Chaos.*** In the bifurcation diagram shown in Fig. 6(b), representing a horizontal section for $\varepsilon = 13\ \text{min}^{-1}$ in the diagram of Fig. 5(c), complex Ca^{2+} oscillations both appear and disappear by period-doubling, following the Feigenbaum sequence which is one of the best known routes leading to chaos (Bergé *et al.*, 1984). The chaotic region contains narrow windows of periodicity. This bifurcation diagram is qualitatively similar to the one obtained by Shen and Larter (1995) in a different model for complex Ca^{2+} oscillations. However, a major quantitative difference between the two diagrams pertains to the range of stimulation levels in which com-

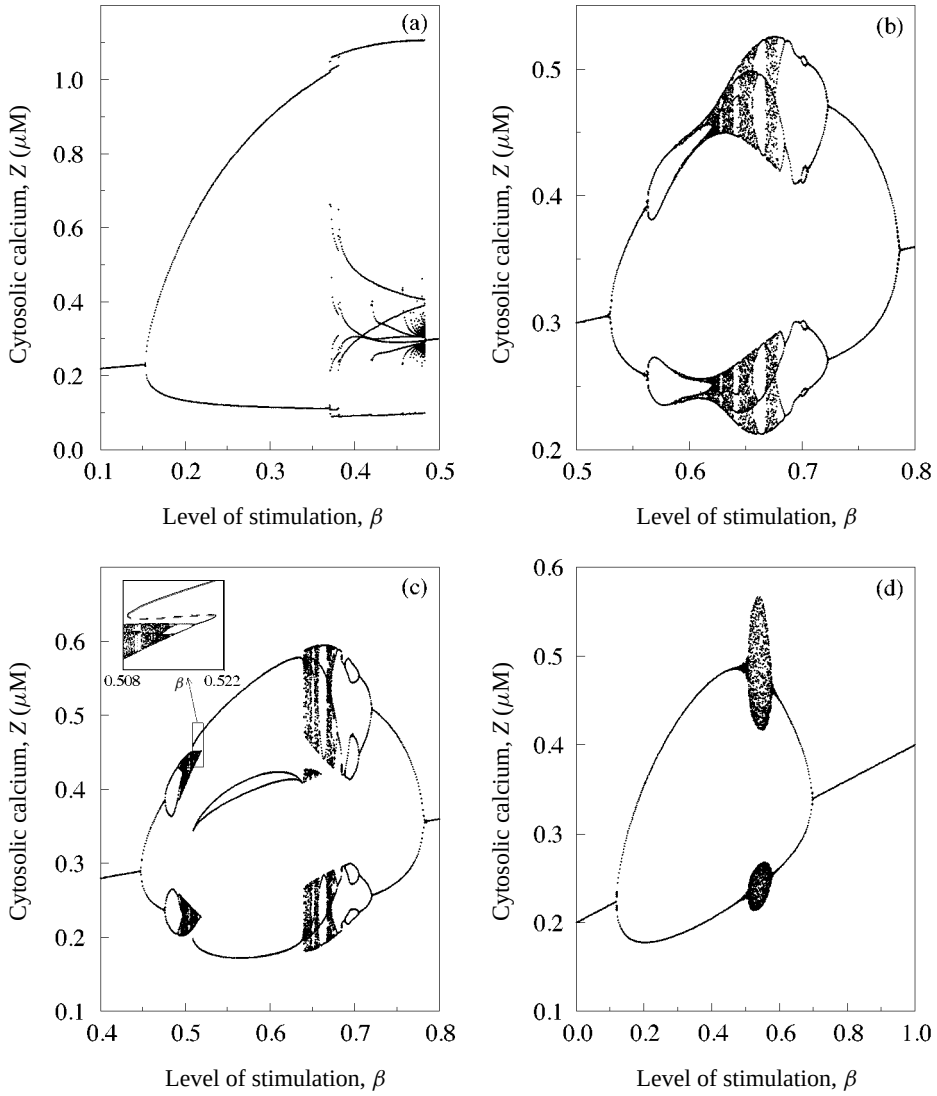

Figure 6. Bifurcation diagrams showing the appearance and disappearance of (a) bursting, (b) chaos, (c) chaos and birhythmicity and (d) quasiperiodicity as a function of β. These diagrams have been established by numerical integration of equations (1)–(5) for the same parameter values as in Figs 4 and 5. (a) Corresponds to the section (dashed line) shown in Fig. 5(a). (b) and (c) Correspond to the sections (dashed lines) shown in Fig. 5(c) for $\varepsilon = 13$ min^{-1} and $\varepsilon = 11$ min^{-1}, respectively. (d) Corresponds to the section (dashed line) shown in Fig. 5(b).

plex oscillations occur: this range, which here extends from $\beta = 0.61$ to 0.68, is at least ten times larger in the present model. For some other parameter values, regions of bursting and chaos can both be observed in the same bifurcation diagram established as a function of β (data not shown).

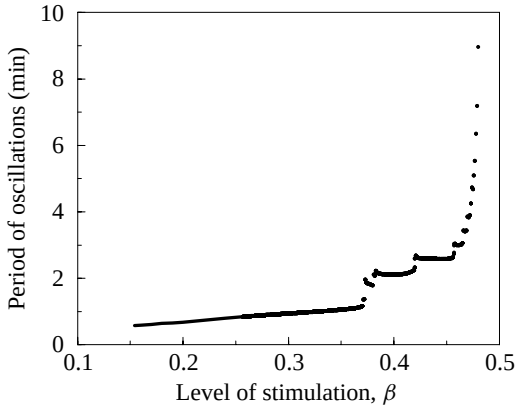

Figure 7. Relationship between the period of Ca^{2+} oscillations and the level of stimulation for a set of parameter values corresponding to oscillations of the bursting type. Parameter values are the same as in Fig. 4(a) and (d) and Fig. 5(a). At the right extremity of the oscillatory domain ($\beta = 0.483$), the period tends to infinity, which denotes the existence of a homoclinic bifurcation.

5.3. ***Birhythmicity.*** With the same set of parameter values as in Fig. 6(b), except for ε which is slightly smaller ($\varepsilon = 11$ min^{-1} instead of 13 min^{-1}), one can observe birhythmicity in the bifurcation diagram [Fig. 6(c), see also Fig. 5(c)]. This behavior corresponds to the coexistence of two stable limit cycles for the same values of the parameters. Here, birhythmicity arises by a phenomenon of hysteresis involving multiple branches of oscillatory behavior separated by an unstable limit cycle, between the two limit points in $\beta = 0.509$ and $\beta = 0.521$ [see inset to Fig. 6(c), illustrating for the maxima of Z the coexistence between the two types of stable oscillations]. For stimulation levels between $\beta = 0.509$ and $\beta = 0.518$, oscillations coexist with a chaotic regime. Between $\beta = 0.518$ and $\beta = 0.521$, two stable limit cycles coexist. These two limit cycles are represented simultaneously in Fig. 8, where (a) represents the temporal evolution of cytosolic Ca^{2+} and (b) the two limit cycles in the phase plane (Z, Y). The two stable cycles are shown for $\beta = 0.520$ in Fig. 8(b), together with the corresponding oscillations in Z [Fig. 8(a)].

The unstable cycle [dashed line in the inset to Fig. 6(c)] separates the attraction basins of the two stable oscillatory regimes. Thus, as illustrated in Fig. 9, when starting from the simple periodic oscillations in the case of Fig. 8, a perturbation in the form of a small increase in cytosolic Ca^{2+} (Z) will cause a transition to the periodic oscillations with a small shoulder. Numerical simulations indicate that the attraction basin of the small cycle is much more reduced than that of the larger cycle.

Furthermore, a phenomenon of period-adding is also seen in $\beta = 0.509$ in the bifurcation diagram shown in Fig. 6(c): periodic Ca^{2+} oscillations with a small shoulder (corresponding to the appearance of an additional intermediate pair of maxima and minima in Z) can be observed from $\beta = 0.509$ (where they coexist with

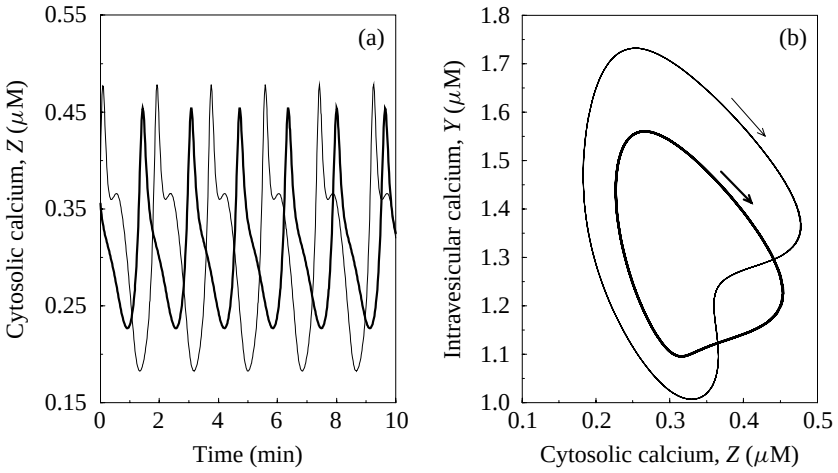

Figure 8. (a) Temporal evolution of cytosolic Ca^{2+} and (b) limit cycles in the (Z, Y) phase plane for the two stable coexisting cycles in the region of birhythmicity. The curves are obtained by numerical integration of equations (1)–(5), starting from different initial conditions. Parameter values are those listed in the second column of Table 1, except for β which is equal to 0.52 and ε which is equal to 11 min^{-1}.

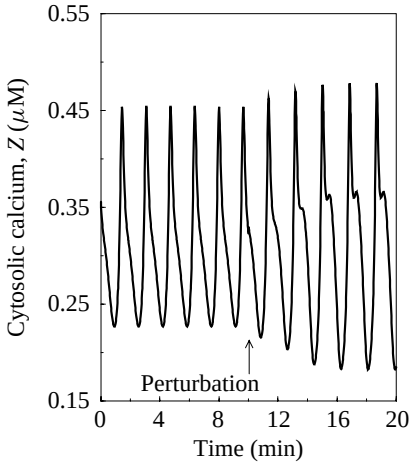

Figure 9. Transition between two types of coexisting, periodic oscillations following a small increase in the cytosolic Ca^{2+} level from 0.322 μM to 0.330 μM in the conditions of birhythmicity. Parameter values are the same as in Fig. 8.

chaotic oscillations) to 0.640, at which value another domain of chaotic oscillations begins.

5.4. ***Quasiperiodicity.*** Quasiperiodic oscillations appear and disappear through a torus bifurcation in which the limit cycle undergoes a secondary Hopf bifurcation, as shown in Fig. 6(d), which represents a section (dashed line) through the diagram of Fig. 5(b). For this reason, the system now possesses two natural incommensurable

frequencies. Thus, the trajectories in the phase space tend to cover a torus, as can be seen in Fig. 4(f).

6. CHARACTERIZATION OF COMPLEX OSCILLATIONS

The various types of complex oscillations are hardly distinguishable from the sole examination of the time series and the associated phase space attractors. Several methods have been developed to characterize these behaviors (Bergé *et al*., 1984). In a first step, we have characterized bursting, chaos and quasiperiodic oscillations by use of Poincaré sections. This has been done for the three cases listed in Table 1, corresponding to the examples of bursting, chaos, and quasiperiodicity illustrated in Fig. 4. We have also obtained the power spectra associated with these three types of oscillations. Finally, the Lyapounov exponents used to characterize the sensitivity to initial conditions (and thus to indicate the presence of chaos) have been obtained over the whole range of possible β values, in each of the three cases considered in Fig. 4.

6.1. ***First return maps.*** To build first return maps, we plot the maximum value of one variable of the system (here Z, the cytosolic Ca^{2+} concentration) as a function of the value of its preceding maximum. We have performed such an analysis, and have plotted in Fig. 10 the results obtained when considering various numbers of successive maxima in cytosolic Ca^{2+}: 5 (first row), 10 (second row), 20 (third row) and 100 (fourth row). In the case of simple, regular oscillations, such a map consists of a single point. For complex oscillations, as can be seen in Fig. 10 there is a clear distinction between the three return maps corresponding to bursting, chaos or quasiperiodicity in the model considered for complex Ca^{2+} dynamics. In the case of bursting (Fig. 10, first column), the map consists of five points, reflecting the number of peaks per period obtained for the particular set of parameter values considered. In the case of chaos (Fig. 10, second column), the map tends to be continuous, with an inverted bell-shaped form, resembling that found for a large variety of chaotic systems. Finally, for the quasiperiodic oscillations (Fig. 10, third column), the map takes the form of a closed curve. The use of first return maps thus appears to be most appropriate for distinguishing between the different types of complex oscillatory behavior. Figure 10 indicates, however, that a minimum number of successive maxima must be used to reach unambiguous conclusions. Thus, in Fig. 10, the asymptotic shape (bottom row) of the return map for chaos and quasiperiodicity begins to be distinguishable for a time series containing 10 peaks, but the picture becomes clearer when 20 maxima are considered.

6.2. ***Power spectra.*** Figure 11 represents the Fast Fourier Transform (Garcia, 1994) of the various temporal data shown in Fig. 4. For bursting [Fig. 11(a)], we can distinguish the natural frequencies of the system [in the case considered,

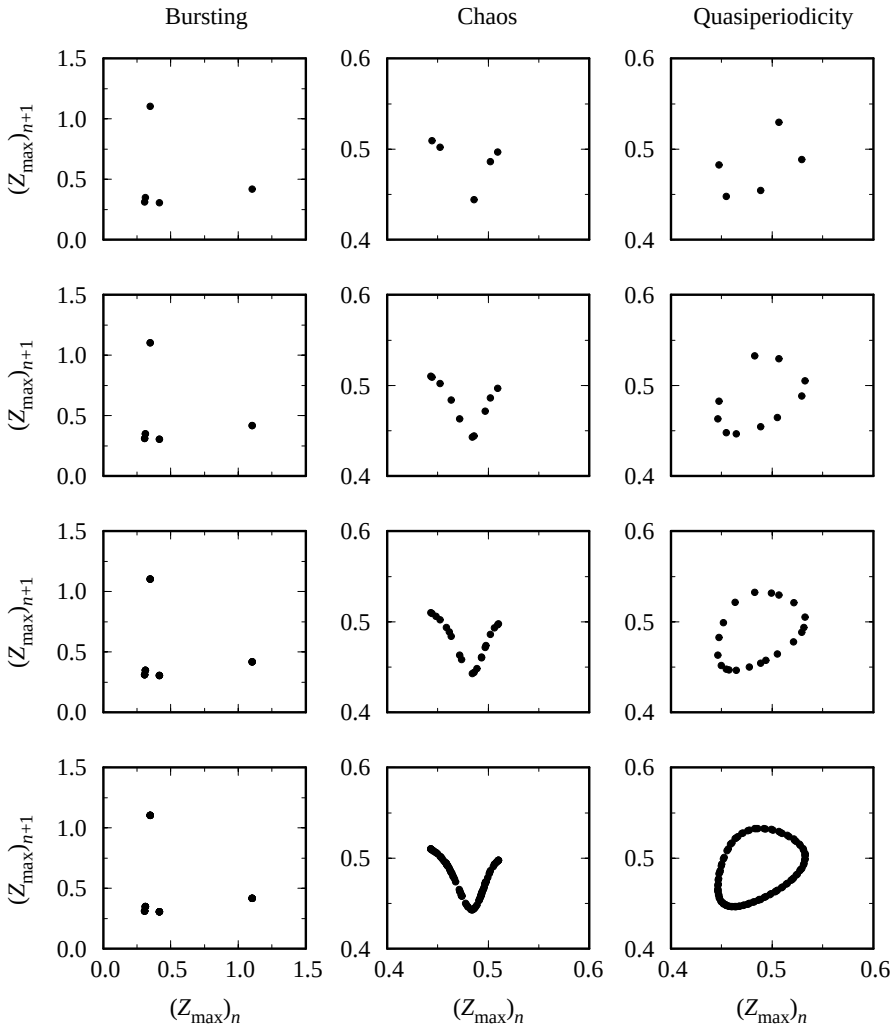

Figure 10. Characterization of complex Ca^{2+} oscillations by means of first return maps. Shown are the return maps obtained for bursting (column 1); chaos (column 2); and quasiperiodicity (column 3) for time series containing 5 (row 1), 10 (row 2), 20 (row 3) and 100 (row 4) successive maxima in cytosolic Ca^{2+} (Z). For each return map, the value of the $(n+1)$th peak in Z is plotted versus the nth peak value. Results have been obtained numerically in the same conditions as (a)–(c) in Fig. 4.

all the lines are multiples of 0.33 min^{-1}, which is the smallest natural frequency, corresponding to the period of the bursting oscillations shown in Fig. 4(a)]. These natural frequencies are combined in the spectrum with their harmonics. For the chaotic dynamics [Fig. 4(b)], the spectrum [Fig. 11(b)] takes a continuous form, with a larger peak which is reminiscent of the frequency ν_{CL} of the unstable limit cycle from which chaos originates (this frequency is obtained by mean of AUTO as $\nu_{CL} = 0.745\ min^{-1}$). The quasiperiodic spectrum [Fig. 11(c)] corresponding to the

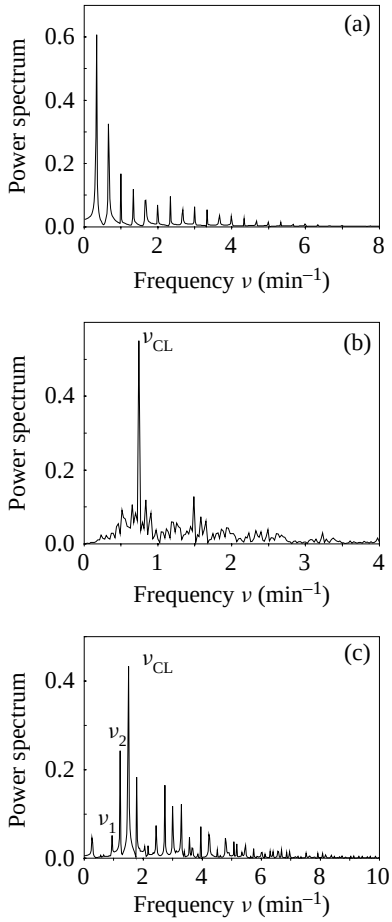

Figure 11. Power spectra corresponding to the three types of complex Ca^{2+} oscillations shown in Fig. 4. (a) Bursting; (b) chaos; (c) quasiperiodicity. Results have been obtained by computing the square of the Fourier transform of the time evolution of Z using a Fast Fourier Transform method (FFT).

oscillations of Fig. 4(c) allows us to determine the two natural frequencies of the system, which are incommensurable. The highest line in fact corresponds to the frequency of the unstable limit cycle (given by AUTO as $\nu_{CL} \sim 1.506\,\mathrm{min}^{-1}$) which originates from the first Hopf bifurcation. The second and the third lines are the two natural frequencies of the system ($\nu_1 = 0.953\ \mathrm{min}^{-1}$ and $\nu_2 = 1.221\ \mathrm{min}^{-1}$), while the first line corresponds to the difference $\nu_2 - \nu_1 = 0.268\ \mathrm{min}^{-1}$. The ratio between these two natural frequencies is an irrational number close to 1.281.

6.3. ***Lyapounov exponents.*** A chaotic regime is characterized by the intrinsic unpredictability of its time evolution, since two trajectories, initially indistinguishable, will diverge exponentially in the course of time. To analyse qualitatively and quantitatively the dynamics of the system, it is useful to compute the Lyapounov

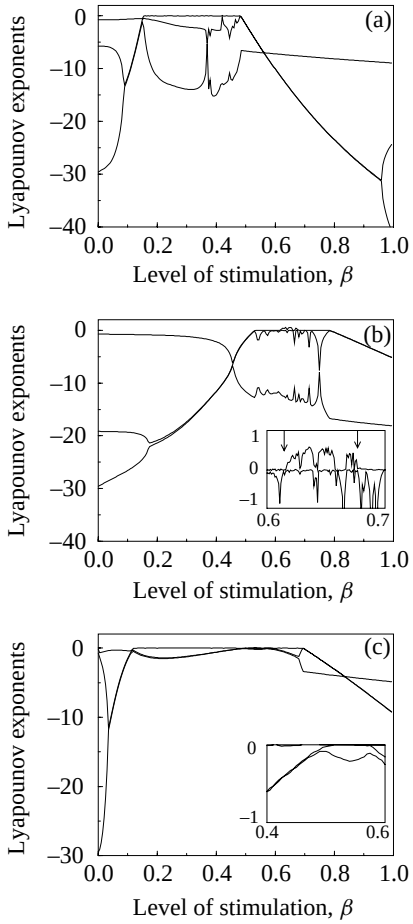

Figure 12. Characterization of the three types of complex Ca^{2+} oscillations shown in Fig. 4 by computing their Lyapounov exponents (see text). Results have been obtained by using the algorithm of Wolf *et al.* (1985).

exponents, which reflect the mean rate of divergence of trajectories initially close in the phase space. Because our system is dissipative, the sum of the three exponents must remain negative (Bergé *et al.*, 1984). The various attractors can be distinguished qualitatively by means of the sign of their Lyapounov exponents. We have determined the Lyapounov exponents characterizing the dynamics of the system over the whole range $\beta = 0$ to 1. As shown by the bifurcation diagrams of Fig. 6, complex oscillations of the bursting, chaotic or quasiperiodic types only occur in windows of β values.

In the case of bursting [Fig. 12(a)], only one exponent goes to zero, while the other two remain negative. This means that every perturbation from the cyclic trajectory in the phase space [Fig. 4(d)] will be damped, except in one direction. For chaotic dynamics [Fig. 12(b)], one Lyapounov exponent becomes positive [in the interval marked by the two arrows in the inset of Fig. 12(b)], reflecting the fact that in

this direction, two initially very slightly different trajectories will move apart; this phenomenon corresponds to the well-known sensitivity to initial conditions. In the case of quasiperiodicity [Fig. 12(c)], two exponents are equal to zero while the third one is negative.

7. DISCUSSION

The present study is devoted to a thorough analysis of a model previously proposed for complex Ca^{2+} oscillations, which takes into account both CICR and stimulation by Ca^{2+} of $InsP_3$ degradation by 3-kinase (Borghans *et al*., 1997). This model is realistic as the two types of regulation by Ca^{2+} have been well characterized. The model predicts that although simple periodic Ca^{2+} spiking is expected to be the most commonly observed behavior, complex Ca^{2+} oscillations in the form of bursting or chaos should also be seen in some nonexcitable cell types under appropriate circumstances. Until now, bursting in Ca^{2+} oscillations has only been reported in experimental studies in hepatocytes responding to appropriate stimuli (Capiod *et al*., 1991; Green *et al*., 1993; Dixon *et al*., 1993, 1995; Marrero *et al*., 1994). There exists a high variability in the propensity of different hepatocytes from the same line to display complex oscillations, which holds with the property of the model that the regions of bursting and chaos in parameter space are relatively small. The fact that these regions are much smaller than those of simple regular Ca^{2+} spiking furthermore agrees with the experimental observation, that simple periodic Ca^{2+} spiking is much more common than complex Ca^{2+} oscillations.

In the present model, an increase in cytosolic Ca^{2+} has two opposite effects. On one hand, due to CICR, it enhances the release of Ca^{2+} from internal stores. On the other hand, due to 3-kinase stimulation by Ca^{2+}, it brings about a decrease in $InsP_3$, which in turn reduces the rate of Ca^{2+} release into the cytosol. These counteracting effects of Ca^{2+} are the source of bursting and chaos in the present model, because the system somehow behaves as a periodically forced oscillator, for which complex oscillations are known to occur (Strogatz, 1994; Goldbeter, 1996). Indeed, CICR, which can proceed in the presence of a constant level of $InsP_3$, provides a mechanism for autonomous oscillations, while the signal ($InsP_3$) that triggers oscillations is self-modulated, as $InsP_3$ raises the level of cytosolic Ca^{2+}, which in turn decreases that of $InsP_3$ through the action of the Ca^{2+}-activated 3-kinase.

Other mechanisms generating complex Ca^{2+} oscillations have been proposed. Thus, as shown by Shen and Larter (1995), the interplay between CICR and the stimulation of phospholipase C activity by Ca^{2+} might also provide a realistic source for bursting and chaos in Ca^{2+} signaling. However, in that model, complex Ca^{2+} oscillations only arise in a very small region of the parameter space, for example, between $\beta = 0.600$ and $\beta = 0.628$ (chaos occurs over an even smaller range of β values). Moreover, in contrast to the present results and to what is seen in hepatocytes, the pattern of Ca^{2+} bursting obtained by Shen and Larter predicts

that Ca^{2+} always returns to it basal level between successive spikes. Bursting was also theoretically predicted in models involving the Ca^{2+}-induced inactivation of the $InsP_3R$ or the interplay between distinct Ca^{2+}- and $InsP_3$-sensitive Ca^{2+} pools (Borghans *et al*., 1997). An inhibitory role of protein kinase C (PKC) in the origin of bursting in hepatocytes has been stressed by Dixon *et al*. (1993, 1995) on the basis of their experimental observations. According to these authors, this variety in temporal patterns could arise because of differences in the negative feedback exerted by PKC on G proteins coupled to the receptors. Such a regulation was incorporated in a model for Ca^{2+} bursting (Chay *et al*., 1995), based on the activation of PLC by Ca^{2+} coupled to both the indirect inhibition of the enzyme by PKC (itself activated by Ca^{2+}) and the Ca^{2+}-induced inactivation of the $InsP_3$-sensitive Ca^{2+} channel.

Complex Ca^{2+} oscillations of the bursting type are easily recognizable by the very appearance of the time evolution of the cytosolic Ca^{2+} level. In contrast, chaotic dynamics could be harder to distinguish from simple periodic oscillations. The analysis performed here suggests that, provided that the available time series is sufficiently long, the construction of first return maps should be the most straightforward method to distinguish periodic oscillations from aperiodic ones. Based on such return maps, preliminary analysis of some experimental time series of Ca^{2+} oscillations, obtained in pancreatic acinar cells and hepatocytes, led to the conclusion that these time series could result from chaotic dynamics (Strizhak *et al*., 1995). However, it should be kept in mind that to perform such an analysis based on return maps, sufficiently long experimental time series must be obtained in constant conditions, with a short sampling time and a low standard deviation. Our results indicate (see Fig. 10) that a time series containing from 10 to 20 successive maxima already allows one to distinguish between the various types of oscillatory behavior, but the longer the time series, the more unambiguous are the conclusions.

The physiological significance of aperiodic Ca^{2+} oscillations such as those shown in Fig. 4(b) might be rather weak, both because they do not differ much from simple periodic oscillations and because they would be rather unstable with respect to small variations in the cellular parameters, given that the domain of chaos is much smaller than that of periodic oscillations in parameter space. The present results as well as those obtained in related models show, however, that well-known properties of intracellular Ca^{2+} signaling can readily generate complex Ca^{2+} oscillations, including chaos.

As to Ca^{2+} oscillations of the bursting type, the plateau phase during which Ca^{2+} remains elevated for a rather long period of time could serve to activate slower, Ca^{2+}-dependent processes. The possible physiological significance of oscillations of the bursting type is supported by the fact that such oscillations are reminiscent of those seen in electrically excitable cells, in which complex oscillations arise from the interplay between a plasma-membrane oscillator and the $InsP_3R$ (Chay, 1993b, 1997; Keizer and De Young, 1993; Li *et al*., 1994; Chay *et al*., 1995). In such cells, it is known that cellular processes are activated differently by Ca^{2+}

spiking or bursting; thus, in pancreatic β cells, granular exocytosis is optimized by long-duration Ca^{2+} bursting (Rorsman and Trube, 1986; Pipeleers, 1987).

Further experimental investigation of complex Ca^{2+} oscillatory dynamics would be of great value, both because it might reveal important features concerning the regulatory mechanisms underlying such Ca^{2+} oscillations, and because of the potential physiological significance of the phenomenon. Together with the theoretical results obtained in other models, the present work suggests that complex Ca^{2+} oscillations should be more widespread than usually thought. Our results point to self-modulation of the $InsP_3$ stimulus as a potential mechanism for generating bursting and chaos in Ca^{2+} signaling.

ACKNOWLEDGMENTS

This work was supported by the programme 'Actions de Recherche Concertée' (ARC 94-99/180) launched by the Division of Scientific Research, Ministry of Science and Education, French Community of Belgium. G. Houart holds a research fellowship from the 'Fonds pour la formation à la Recherche dans l'Industrie et dans l'Agriculture'. G. Dupont is 'Chercheur Qualifié du Fonds National de la Recherche Scientifique'.

REFERENCES

Bergé, P., Y. Pomeau and C. Vidal (1984). *Order within Chaos: Towards a Deterministic Approach to Turbulence*, New York: Wiley.

Berridge, M. J. (1993). Inositol trisphosphate and calcium signalling. *Nature* **361**, 315–325.

Berridge, M. J. (1997). Elementary and global aspects of calcium signalling. *J. Physiol.* **499**, 291–306.

Berridge, M. J. and G. Dupont (1994). Spatial and temporal signalling by calcium. *Curr. Opin. Cell Biol.* **6**, 267–274.

Borghans, J. A. M., G. Dupont and A. Goldbeter (1997). Complex intracellular calcium oscillations: a theoretical exploration of possible mechanisms. *Biophys. Chem.* **66**, 25–41.

Capiod, T., J. Noel, L. Combettes and M. Claret (1991). Cyclic AMP-evoked oscillations of intracellular [Ca^{2+}] in guinea-pig hepatocytes. *Biochem. J.* **275**, 277–280.

Chay, T. R. (1993a). Modelling for nonlinear dynamical processes in biology, in *Patterns, Information and Chaos in Neuronal Systems*, B. J. West (Ed.), River Edge, NJ: World Scientific Publishing, pp. 73–122.

Chay, T. R. (1993b). The mechanism of intracellular Ca^{2+} oscillation and electrical bursting in pancreatic β-cells. *Adv. Biophys.* **29**, 75–103.

Chay, T. R. (1997). Effects of extracellular calcium on electrical bursting and intracellular and luminal calcium oscillations in insulin secreting pancreatic β-cells. *Biophys. J.* **73**, 1673–1688.

Chay, T., Y. S. Fan and Y. S. Lee (1995). Bursting, spiking, chaos, fractals, and universality in biological rythms. *Int. J. Bifurcation Chaos* **5**, 595–635.

De Smedt, F., L. Missiaen, J. B. Parys, V. Vanweyenberg, H. De Smedt and C. Erneux (1997). Isoprenylated human brain type I inositol 1,4,5-trisphosphate 5-phosphatase controls Ca^{2+} oscillations induced by ATP in chinese hamster ovary cells. *J. Biol. Chem.* **204**, 17367–17375.

Dixon, C. J., P. H. Cobbold and A. K. Green (1993). Adenosine 5′-[$\alpha\beta$-methylene] triphosphate potentiates the oscillatory cytosolic Ca^{2+} responses of hepatocytes to ATP, but not to ADP. *Biochem. J.* **293**, 757–760.

Dixon, C. J., P. H. Cobbold and A. K. Green (1995). Oscillations in cytosolic free Ca^{2+} induced by ADP and ATP in single rat hepatocytes display differential sensitivity to application of phorbol ester. *Biochem. J.* **309**, 145–149.

Doedel, E. J. (1981). A program for the automatic bifurcation analysis of autonomous systems. *Congr. Num.* **30**, 265–284.

Dolmetsch, R. E., K. Xu and R. S. Lewis (1998). Calcium oscillations increase the efficiency and specificity of gene expression. *Nature* **392**, 933–936.

Dupont, G. (1999). Spatio-temporal organisation of intracellular calcium signals: from experimental to theoretical aspects. *Comments Theor. Biol.* In press.

Dupont, G. and C. Erneux (1997). Simulations of the effect of inositol 1,4,5-trisphosphate 3-kinase and 5-phosphatase activities on Ca^{2+} oscillations. *Cell Calcium* **22**, 321–331.

Dupont, G. and A. Goldbeter (1992). Oscillations and waves of cytosolic calcium: insights from theoretical models. *BioEssays* **14**, 485–493.

Dupont, G. and A. Goldbeter (1993). One-pool model for Ca^{2+} oscillations involving Ca^{2+} and inositol 1,4,5-trisphosphate as co-agonists for Ca^{2+} release. *Cell Calcium* **14**, 311–322.

Endo M., M. Tamaka and Y. Ogawa (1970). Calcium induced release of calcium from the sarcoplasmic reticulum of skinned skeletal muscle cells. *Nature* **288**, 34–36.

Fabiato A. and F. Fabiato (1975). Contractions induced by a calcium-triggered release of calcium from the sarcoplasmic reticulum of single skinned cardiac cells. *J. Physiol. (London)* **249**, 469–495.

Garcia, A. L. (1994). *Numerical Methods for Physics*, Englewood Cliffs, NJ: Prentice Hall.

Goldbeter, A. (1996). *Biochemical Oscillations and Cellular Rhythms*, Cambridge: Cambridge University Press.

Green, A. K., P. H. Cobbold and C. J. Dixon (1994). Elevated intracellular cyclic AMP exerts different modulatory effects on cytosolic free Ca^{2+} oscillations induced by ADP and ATP in single rat hepatocytes. *Biochem. J.* **302**, 949–955.

Green, A. K., C. J. Dixon, A. G. MacLennan, P. H. Cobbold and M. J. Fisher (1993). Adenine dinucleotide-mediated cytosolic free Ca^{2+} oscillations in single hepatocytes. *FEBS Lett.* **322**, 197–200.

Keizer, J. and G. De Young (1992). Two roles for Ca^{2+} in agonist stimulated Ca^{2+} oscillations. *Biophys. J.* **61**, 649–660.

Keizer, J. and G. De Young (1993). Effect of voltage-gated plasma membrane Ca^{2+} fluxes on IP_3-linked Ca^{2+} oscillations. *Cell Calcium* **14**, 397–410.

Li, W.-H., J. Llopis, M. Whitney, G. Zlokarnik and R. Y. Tsien (1998). Cell-permeant caged $InsP_3$ ester shows that Ca^{2+} spike frequency can optimize gene expression. *Nature* **392**, 936–941.

Li, Y. X., J. Rinzel, J. Keizer and S. S. Stojilkovic (1994). Calcium oscillations in pituitary gonadotrophs: comparison of experiment and theory. *Proc. Natl. Acad. Sci. USA* **91**, 58–62.

Mailleux, P., K. Takazawa, C. Erneux and J.-J. Vanderhaeghen (1991). Inositol 1,4,5-

trisphosphate 3-kinase distribution in the rat brain. High levels in the hippocampus CA1 pyramidal and cerebellar Purkinje cells suggest its involvement in some memory processes. *Brain Res.* **539**, 957–962.

Marrero, I., A. Sanchez-Bueno, P. H. Cobbold and C. J. Dixon (1994). Taurolithocholate and thaurolithocholate 3-sulfate exert different effects on cytosolic free Ca^{2+} concentration in rat hepatocytes. *Biochem. J.* **300**, 383–386.

Meyer, T. and L. Stryer (1988). Molecular model for receptor-stimulated calcium spiking. *Proc. Natl. Acad. Sci. USA* **85**, 5051–5055.

Ozil, J. P. and K. Swann (1995). Stimulation of repetitive calcium transients in mouse eggs. *J. Physiol.* **483**, 331–346.

Pipeleers, D. (1987). The biosociology of pancreatic β cells. *Diabetologia* **30**, 277–291.

Renard, D., J. Poggioli, B. Berthon and M. Claret (1987). How far does phospholipase C depend on the cell calcium concentration? *Biochem. J.* **243**, 391–398.

Rorsman, P. and G. Trube (1986). Calcium and delayed potassium currents in mouse pancreatic β-cells under voltage-clamp conditions. *J. Physiol. (London)* **374**, 531–550.

Shen, P. and R. Larter (1995). Chaos in intracellular Ca^{2+} oscillations in a new model for non-excitable cells. *Cell Calcium.* **17**, 225–232.

Sneyd, J., J. Keizer and M. Sanderson (1995). Mechanisms of calcium oscillations and waves: a quantitative analysis. *FASEB J.* **9**, 1463–1472.

Strizhak, P., I. S. Magura, K. B. Yatsimirskii and A. I. Masyuk (1995). Return map approach to description of the deterministic chaos in cytosolic calcium oscillations. *J. Biol. Phys.* **21**, 233–239.

Strogatz, S. H. (1994). *Nonlinear Dynamics and Chaos*, Reading, MA: Addison-Wesley.

Takazawa, K., M. Lemos, A. Delvaux, C. Lejeune, J. E. Dumont and C. Erneux (1990). Rat brain inositol 1,4,5-trisphosphate 3-kinase. Ca^{2+}-sensitivity, purification and antibody production. *Biochem. J.* **268**, 213–217.

Takazawa, K., H. Passareiro, J. E. Dumont and C. Erneux (1989). Purification of bovine brain inositol 1,4,5-trisphosphate 3-kinase. Identification of the enzyme by sodium dodecyl sulphate/polyacrylamide-gel electrophoresis. *Biochem. J.* **261**, 483–488.

Tang, Y., J. L. Stephenson and H. G. Othmer (1996). Simplification and analysis of models of calcium dynamics based on IP_3-sensitive calcium channel kinetics. *Biophys. J.* **70**, 246–263.

Thomas, A. P., G. S. Bird, G. Hajnoczky, L. D. Robb-Gaspers and J. W. Putney, Jr. (1996). Spatial and temporal aspects of cellular calcium signaling. *FASEB J.* **10**, 1505–1517.

Verjans, B., R. Lecocq, C. Moreau and C. Erneux (1992). Purification of bovine brain inositol 1,4,5- trisphosphate 5-phosphatase. *Eur. J. Biochem.* **204**, 1083–1087.

Wakui, M., B. V. Potter and O. H. Petersen (1989). Pulsatile intracellular calcium release does not depend on fluctuations in inositol trisphosphate concentration. *Nature* **339**, 317–320.

Wolf, A., J. B. Swift, H. L. Swinney and J. A. Vastano (1985). Determining Lyapunov exponents from a time series. *Physica* **16D**, 285–317.

Received 19 July 1998 and accepted 22 December 1998